

Optomechanically induced transparency in a multi-cavity system subjected to two-level atomic ensemble interference

Gongtao Yu

Anhui University of Science and Technology

Guixia Pan

77935409@qq.com

Anhui University of Science and Technology

Research Article

Keywords: Optomechanically induced transparency, Multi-cavity optomechanical system, Nanomechanical resonators, Hamiltonian, Langevin equations

Posted Date: January 17th, 2024

DOI: <https://doi.org/10.21203/rs.3.rs-3863314/v1>

License: © ⓘ This work is licensed under a Creative Commons Attribution 4.0 International License.

[Read Full License](#)

Additional Declarations: No competing interests reported.

Optomechanically induced transparency in a multi-cavity system subjected to two-level atomic ensemble interference

Gongtao Yu¹ and Guixia Pan^{1,*†}

¹School of Mechanics and Optoelectronic Physics, Anhui University of Science and Technology, Taifen Street, Huainan, 232001, Anhui Province, China.

Contributing authors: 2280250661@qq.com; 77935409@qq.com;

[†]These authors contributed equally to this work.

Abstract

We investigate a hybrid multi-cavity optomechanical system with interference from a two-level atomic ensemble. The system is composed of three optical cavities and two nanomechanical resonators. A two-level atomic ensemble is filled into the middle optical cavity. The optical cavity located in the middle has two interaction forces with the two outermost optical cavities. What is more, the system also includes various types of interaction relations, which are the couplings of optical cavities with mechanical resonators and the coupling of optical cavity with two-level atomic ensemble. In order to study the optical response of optomechanically induced transparency, we modulate the interaction intensity within the system to obtain different electromagnetic induced transparent phenomena. It has been found that under the influence of different parameters, the number of transparent windows and the width of transparent windows increase with an increase in the coupling of the optical cavities with atomic ensemble. In addition, as the system parameters change, the transparency points also move. The position of the two outermost transparent points becomes farther apart when the coupling of optical cavity with mechanical resonators increases. Our approach provides a great flexibility for controlling electromagnetically induced transparency. It will have the great potential applications for quantum information processing.

Keywords: Optomechanically induced transparency, Multi-cavity optomechanical system, Nanomechanical resonators, Hamiltonian, Langevin equations

1 Introduction

Cavity optomechanics (COM) (Bhattacharya et al.2008; Wu et al.2021; Kharel et al.2022; Arregui et al.2023; Ling et al.2021) as a breakthrough in the direction of quantum information in the new era, it has received extensive attention from many researchers. For instance, intermittent chaos induced by radiation-pressure nonlinearity (Zhang et al.2020), the transport of thermal phonons (Wu et al.2021), optical bistability (Sarma et al.2016). It uses the energy of radiation pressure to influence the interaction between the cavity field and the charged mechanical resonator (Lai et al.2018). Recent studies have shown that COM has applications such as quantum interference (Zeng et al.2019) and optomechanical force-sensing (Gebremariam et al.2020). Optomechanically induced transparency (OMIT) (Yan et al.2020; Lai et al.2020; Hao et al.2022; Zhang et al.2018; Lu et al.2018) is a common physical phenomenon in quantum information. It is an optical response caused by interference cancellation of the system. It can be used to control the speed of light (Safavi et al.2011; Chen et al.2011; Akram et al.2015), generate quantum entanglement (Zhang et al.2021a; Pan et al.2020), signal amplification (Lu et al.2019) and other directions (Zhang et al.2012; Agarwal et al.2012). Moreover, OMIT provides a new way to study the quantum characteristics of the optical cavity.

As we know, two-level atomic ensemble (Lembessis et al.2021; Jing et al.2021; Vlasiuk et al.2023; Liu et al.2022) has become an important part of the development of cavity dynamics. Through the scientific research of quantum states of two-level atomic ensemble, the phenomenon of spontaneous radiation of atoms ensemble has been well explained (Kien et al.2017). The spontaneous radiation intensity of a single atomic ensemble is relatively weak (Kuraptsev et al.2014), and it only has a strong atomic ensemble radiation phenomenon when it is coupled with the cavity field. In addition, quantum effects between optical cavities and two-level atomic ensemble under the condition of full quantization are the focus of current research. Hisaki et al. (Oka et al.2005) proposes a quantum phase gate model with two-level atomic ensemble. They use the finite-difference time-domain method and the optical Bloch equation to perform a semi-classical analysis of the optical response obtained by the model system. The Fano resonance and slow light phenomena in two-level atomic ensemble coupled opto-mechanical systems are discussed (Jiang et al.2017). They found that the group delay of the transmitting probe field is inversely related to the decay rate of the qubit.

In recent years, the exploration of OMIT has become a hot spot in the development of quantum theory. OMIT and traditional EIT (Zhang et al.2021b; Zheng et al.2023; Oliveira et al.2021; Yang et al.2022) have many similar nonlinear characteristics, and they are the main embodiments of nonlinear optical effects. The research scope of scholars is not limited by OMIT, the attention of double-OMIT (Ma et al.2014; Lu et al.2019; Gu et al.2014) and multiple-OMIT (Lai et al.2020; Huang et al.2014; Xiao et al.2015) are also increasing. Ma et al. (Ma et al.2014) observed the double-OMIT effect by controlling the intensity of Coulomb action. They also studied the relationship between Coulomb intensity and transparent window splitting. Lai et al. (Lai et al.2020) introduced dark mode effect of opto-mechanical system to simulate multiple-OMIT. The research results have certain reference significance for information storage in the optical communication process.

In this work, we propose a model of a multi-cavity optomechanical system with two-level atomic ensemble. In this system, there are interaction relations between optical cavity a_1 and optical cavity a_2 , between optical cavity a_2 and optical cavity a_3 . The coupling strengths between them are J_1 and J_2 . For optical cavity a_2 , it is driven by a strong pump and a weak probe field (Hamedi et al.2022), and the two-level atomic ensemble is also coupled with it. At the same time, under the influence of radiation pressure, the optical cavity a_1 on the left is coupled with the charged mechanical resonator b_1 . The optical cavity a_3 is coupled to the charged mechanical resonator b_2 . By adjusting the coupling parameters inside the system, multiple-OMIT phenomena can be observed from the output spectral.

2 Model and Hamiltonion

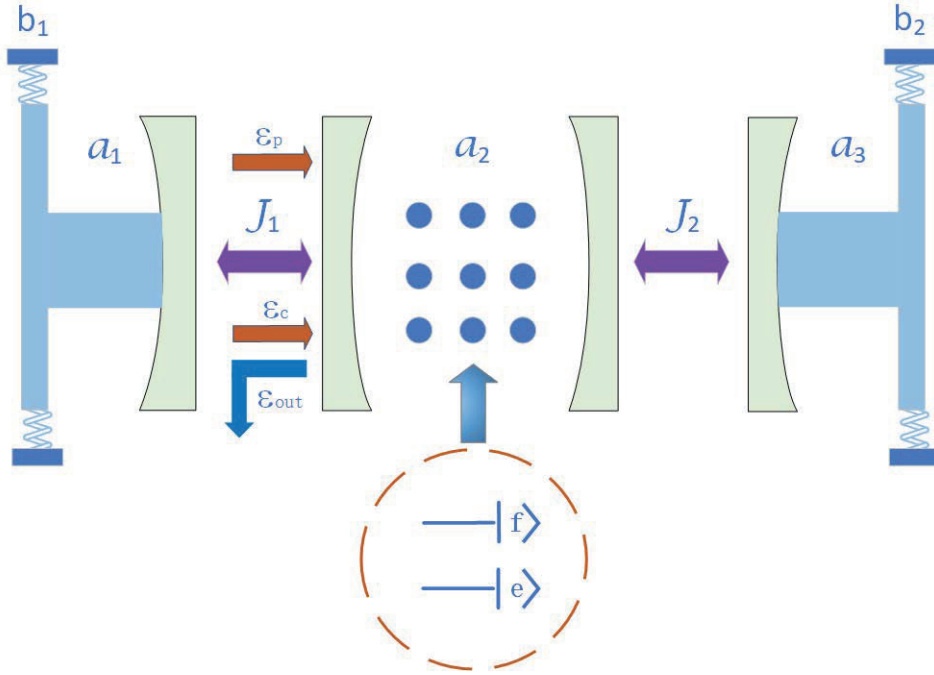


Fig. 1 A schematic diagram of a cavity opto-mechanical system driven by a strong pump field and a weak probe field.

Figure 1 shows the multi-cavity optomechanical system. The system consists of three optical cavities and two nanomechanical resonators. And the two-level atomic ensemble is introduced into the cavity a_2 that is simultaneously driven by a strong pump field with frequency ω_c and a weak probe field with frequency ω_p . Here, $|e\rangle$ and $|f\rangle$ represent atomic ensemble in the ground state and excited state, respectively. And $\omega_{fe} = \omega_f - \omega_e$ is the energy level frequency spacing. Firstly, the optical cavity a_2

is driven by the red detuning effect (Chen et al.2019), and λ describes the coupling strength between the cavity field and two-level atomic ensemble. Secondly, the coupling parameter of the optical cavity a_1 and the charged mechanical resonator b_1 is g_1 . Furthermore, the coupling constant between the optical cavity a_3 and the charged mechanical resonator b_2 is g_2 . Last but not least, we consider the dipole approximation and spin wave approximation (Watanabe et al.2009), the Hamiltonian of the whole system is the sum of three terms

$$\begin{aligned}
H &= H_0 + H_{int} + H_{dr}, \\
H_0 &= \hbar\omega_1 a_1^\dagger a_1 + \hbar\omega_2 a_2^\dagger a_2 + \hbar\omega_3 a_3^\dagger a_3 + \hbar\omega_{m1} b_1^\dagger b_1 \\
&\quad + \hbar\omega_{m2} b_2^\dagger b_2 + \hbar \sum_{n=1}^N \omega_{fe} \sigma_{ff}^{(n)}, \\
H_{int} &= \hbar J_1 (a_1^\dagger a_2 + a_2^\dagger a_1) + \hbar J_2 (a_2^\dagger a_3 + a_3^\dagger a_2) \\
&\quad + \hbar g_1 a_1^\dagger a_1 (b_1^\dagger + b_1) + \hbar g_2 a_3^\dagger a_3 (b_2^\dagger + b_2) \\
&\quad + \hbar \lambda \sum_{n=1}^N (a_2 \sigma_{fe}^{(n)} + a_2^\dagger \sigma_{ef}^{(n)}), \\
H_{dr} &= i\hbar\varepsilon_c (a_2^\dagger e^{-i\omega_c t} - a_2 e^{i\omega_c t}) \\
&\quad + i\hbar\varepsilon_p (a_2^\dagger e^{-i\omega_p t} - a_2 e^{i\omega_p t}). \tag{1}
\end{aligned}$$

The total Hamiltonian of the system is divided into three parts H_0 , H_{int} , H_{dr} . The term H_0 represents the free Hamiltonian of the cavity fields, the charged mechanical resonators and the two-level atomic ensemble. We introduce the creation (annihilation) operators (Kumar et al.2013), a_j^\dagger (a_j , $j = 1, 2, 3$) and b_i^\dagger (b_i , $i = 1, 2$), which correspond to the cavity fields and the mechanical modes. The frequencies of the three cavity fields and the two charged mechanical resonators are denoted by ω_1 , ω_2 , ω_3 , ω_{m1} , and ω_{m2} , respectively. H_{int} represents the interactions of the system. The first and second parts are the interaction energy between the cavity fields and the cavity fields, and the third and fourth parts are the coupling energy between the cavity fields and the charged mechanical resonators. The sum formula gives the energy transfer during the transition of atomic energy levels. The last line H_{dr} reflects the Hamiltonian between the pump field and the probe field in the system. The amplitudes of the two external fields are $\varepsilon_c = \sqrt{\frac{2\kappa_2 P_c}{\hbar\omega_c}}$ and $\varepsilon_p = \sqrt{\frac{2\kappa_2 P_p}{\hbar\omega_p}}$, and the corresponding powers are P_c and P_p , respectively. Considering cavity field noise and damping oscillation (Alford et al.2019), we make the assumptions $\Delta_1 = \omega_2 - \omega_c$, $\Delta_2 = \omega_{fe} - \omega_c$, and $G_A = \lambda\sqrt{N}$. In the large N limit, we utilize a collective low-energy excitations of the atomic ensemble to represent the coupling between the atoms and the cavity field $A = \frac{1}{\sqrt{N}} \sum_{n=1}^N \sigma_{ef}^{(n)}$, which satisfies the bosonic commutation relation $[A, A^\dagger] = 1$. Considering the fluctuation factors of each part, the quantum Langevin equations can be written as

$$\dot{a}_1 = -(\kappa_1 + i\omega_1)a_1 - iJ_1 a_2 - ig_1 a_1 (b_1^\dagger + b_1),$$

$$\begin{aligned}
\dot{a}_2 &= -(\kappa_2 + i\Delta_1)a_2 - iJ_1a_1 - iJ_2a_3 \\
&\quad - iG_A A + \varepsilon_c + \varepsilon_p e^{-i\Delta_p t}, \\
\dot{a}_3 &= -(\kappa_3 + i\omega_3)a_3 - iJ_2a_2 - ig_2a_3(b_2^\dagger + b_2), \\
\dot{b}_1 &= -(\gamma_{m1} + i\omega_{m1})b_1 - ig_1a_1^\dagger a_1, \\
\dot{b}_2 &= -(\gamma_{m2} + i\omega_{m2})b_2 - ig_2a_3^\dagger a_3, \\
\dot{A} &= -(\gamma + i\Delta_2)A - iG_A a_2.
\end{aligned} \tag{2}$$

When $\varepsilon_c \gg \varepsilon_p$, the Heisenberg operators can be expressed in the form of the steady-state mean values plus its small fluctuations, i.e., $a_1 = a_{1s} + \delta a_1$, $a_2 = a_{2s} + \delta a_2$, $a_3 = a_{3s} + \delta a_3$, $b_1 = b_{1s} + \delta b_1$, $b_2 = b_{2s} + \delta b_2$, and $A = A_s + \delta A$. Defining $x_{1s} = b_1^\dagger + b_1$, $x_{2s} = b_2^\dagger + b_2$, $\bar{\Delta}_1 = \omega_1 + g_1 x_{1s}$, and $\bar{\Delta}_3 = \omega_3 + g_2 x_{2s}$. The steady-state values of the equations are

$$\begin{aligned}
a_{1s} &= \frac{iJ_1 a_2}{-(\kappa_1 + i\bar{\Delta}_1)}, \\
a_{2s} &= \frac{\varepsilon_c}{(\kappa_2 + i\Delta_1) + \frac{J_1^2}{(\kappa_1 + i\bar{\Delta}_1)} + \frac{J_2^2}{(\kappa_3 + i\bar{\Delta}_3)} + \frac{G_A^2}{\gamma + i\Delta_2}}, \\
a_{3s} &= \frac{iJ_2 a_2}{-(\kappa_3 + i\bar{\Delta}_3)}, \\
b_{1s} &= \frac{-ig_1 a_1^\dagger a_1}{\gamma_{m1} + i\omega_{m1}}, \\
b_{2s} &= \frac{-ig_2 a_3^\dagger a_3}{\gamma_{m2} + i\omega_{m2}}.
\end{aligned} \tag{3}$$

In order to improve the convenience of calculation, the higher order terms in the operation process can be ignored, and the analytical equations after linearization are as follows

$$\begin{aligned}
\delta \dot{a}_1 &= -(\kappa_1 + i\widetilde{\Delta}_1)\delta a_1 - iJ_1\delta a_2 - iG_1(\delta b_1^\dagger + \delta b_1), \\
\delta \dot{a}_2 &= -(\kappa_2 + i\Delta_1)\delta a_2 - iJ_1\delta a_1 - iJ_2\delta a_3 - iG_A\delta A, \\
\delta \dot{a}_3 &= -(\kappa_3 + i\widetilde{\Delta}_2)\delta a_3 - iJ_2\delta a_2 - iG_2(\delta b_2^\dagger + \delta b_2), \\
\delta \dot{b}_1 &= -(\gamma_{m1} + i\omega_{m1})\delta b_{1s} - i(G_1^*\delta a_1 + G_1\delta a_1^\dagger), \\
\delta \dot{b}_2 &= -(\gamma_{m2} + i\omega_{m2})\delta b_{2s} - i(G_2^*\delta a_3 + G_2\delta a_3^\dagger), \\
\delta \dot{A} &= -(\gamma + i\Delta_2)\delta A - iG_A\delta a_2.
\end{aligned} \tag{4}$$

We make the substitution $\delta\theta_j \rightarrow \delta\theta_j e^{-i\Delta_p t}$ and bring it into the calculation process $\delta a_1 \rightarrow \delta a_1 e^{-i\Delta_p t}$, $\delta a_2 \rightarrow \delta a_2 e^{-i\Delta_p t}$, $\delta a_3 \rightarrow \delta a_3 e^{-i\Delta_p t}$, $\delta b_1 \rightarrow \delta b_1 e^{-i\Delta_p t}$, $\delta b_2 \rightarrow \delta b_2 e^{-i\Delta_p t}$, and $\delta A \rightarrow \delta A e^{-i\Delta_p t}$. Considering $G_1 = g_1 a_{1s}$, $G_2 = g_2 a_{3s}$, $\widetilde{\Delta}_1 = \omega_1 + g_1(b_{1s}^\dagger + b_{1s})$, $\widetilde{\Delta}_2 = \omega_3 + g_2(b_{2s}^\dagger + b_{2s})$, $\omega_{a1} = \widetilde{\Delta}_1 - \Delta_p$, $\omega_{a2} = \widetilde{\Delta}_1 - \Delta_p$,

$\omega_{a3} = \widetilde{\Delta}_2 - \Delta_p$, $\omega_{b1} = \omega_{m1} - \Delta_p$, $\omega_{b2} = \omega_{m2} - \Delta_p$, $\omega_A = \Delta_2 - \Delta_p$, $\omega_{a1} = \omega_{a2} = \omega_{a3} = \omega_{b1} = \omega_{b2} = \omega_A = \delta$.

And we find the steady-state solution of the above equations, i, e., when $\langle \delta \dot{a}_1 \rangle = \langle \delta \dot{a}_2 \rangle = \langle \delta \dot{a}_3 \rangle = \langle \delta \dot{b}_1 \rangle = \langle \delta \dot{b}_2 \rangle = \langle \delta \dot{A} \rangle = 0$, we obtain

$$\delta a_2 = \frac{\varepsilon_p}{\kappa_2 + i\delta + \frac{J_1^2}{\kappa_1 + i\delta + \frac{|G_1|^2}{\gamma_{m1} + i\delta}} + \frac{J_2^2}{\kappa_3 + i\delta + \frac{|G_2|^2}{\gamma_{m2} + i\delta}} + \frac{G_A^2}{\gamma + i\delta}}. \quad (5)$$

Employing the input-output relationship

$$\varepsilon_{out,p} = 2\kappa_2 \delta a_2 - \varepsilon_p. \quad (6)$$

After a straightforward calculation, the transmitted probe field can be redefined as

$$\begin{aligned} \varepsilon_T &= \varepsilon_{out,p} / \varepsilon_p + 1 = 2\kappa_2 \delta a_2 / \varepsilon_p \\ &= \frac{2\kappa_2}{\kappa_2 + i\delta + \frac{J_1^2}{\kappa_1 + i\delta + \frac{|G_1|^2}{\gamma_{m1} + i\delta}} + \frac{J_2^2}{\kappa_3 + i\delta + \frac{|G_2|^2}{\gamma_{m2} + i\delta}} + \frac{G_A^2}{\gamma + i\delta}}. \end{aligned} \quad (7)$$

3 Multi-OMIT in the output field

In this part, according to the above analytical expressions, we select appropriate parameters to study the behavior of OMIT. By observing the absorption and dispersion spectral lines, we can draw many conclusions about OMIT in multi-cavity systems.

In Fig. 2(a), we manipulate all the coupling parameters in the hybrid system so that their values are not zero, which means five interference pathway forms between the pump field and the probe field. In the following, we can see that there are five transparent points in the output spectral line, so the number of OMIT is five, and they are distributed symmetrically in the image. The five OMIT displays that the optomechanical system becomes simulta-neously transparent to the signal field at five different frequencies. The results are the same as those of Sohail et al (Sohail et al.2016).

In Fig. 2(b), we plot the absorption $\text{Re}(\varepsilon_T)$ of the output field. We can observe three transparent points in the absorption spectrum. Obviously, the optical response of OMIT corresponds to three transparent windows, which has been proven in (Wu et al.2016). What is more, the coupling parameter between cavity field a_1 and mechanical vibrator b_1 in the multi-cavity system is zero ($g_1 = 0$). Thus, the internal and external interference factors on the overall properties of the optomechanical system are four.

In Fig. 2(c), three OMIT indicates three OMIT depressions can be generated in the system. And it is consistent with the results of OMIT which was studied by Xiao et al (Xiao et al.2020). In addition, the figure reveals that there are three transparent points appearing in the output spectral line. In the hybrid system, except for the

coupling of the cavity field a_3 and the mechanical oscillator b_2 disappears ($g_2 = 0$), other optical couplings have not effect on the behavior of the transparent windows.

In Fig. 2(d), when the atomic medium in a photomechanical system is absent ($G_A = 0$), one can easily notice that there are four transmission windows. Compared to the case where all the couplings are present, the absence of atoms reduces the transparency window by one, and the transparent window also widens. These results

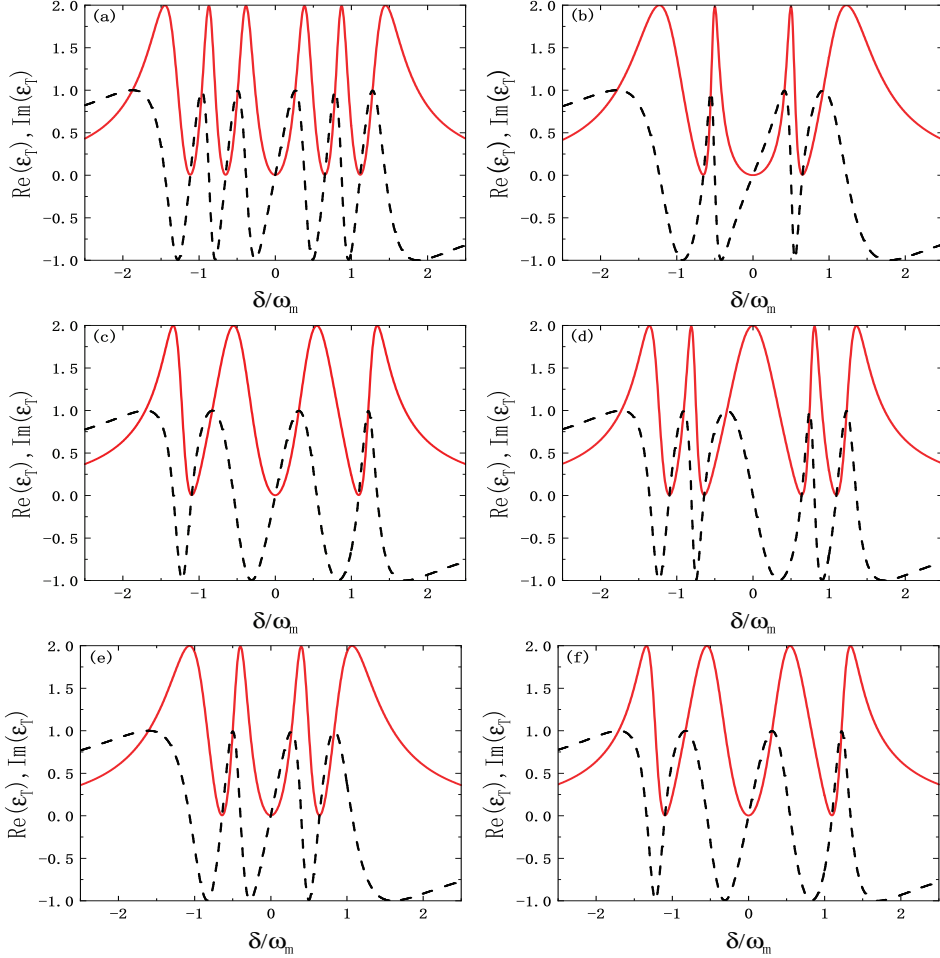


Fig. 2 The figure depicts absorption spectrum $Re(\epsilon_T)$ (solid line) and dispersion spectrum $Im(\epsilon_T)$ (dashed line) in relation to frequency detuning δ/ω_m . (a) $g_1 = 2\pi \times 24 \times 10^3 \text{ Hz}$, $g_2 = 2\pi \times 14 \times 10^3 \text{ Hz}$, $G_A = 2\pi \times 8 \times 10^6 \text{ Hz}$, $J_1 = 2\pi \times 8 \times 10^6 \text{ Hz}$, $J_2 = 2\pi \times 8 \times 10^6 \text{ Hz}$; (b) $g_1 = 0 \text{ Hz}$, $g_2 = 2\pi \times 14 \times 10^3 \text{ Hz}$, $G_A = 2\pi \times 8 \times 10^6 \text{ Hz}$, $J_1 = 2\pi \times 8 \times 10^6 \text{ Hz}$, $J_2 = 2\pi \times 8 \times 10^6 \text{ Hz}$; (c) $g_1 = 2\pi \times 24 \times 10^3 \text{ Hz}$, $g_2 = 0 \text{ Hz}$, $G_A = 2\pi \times 8 \times 10^6 \text{ Hz}$, $J_1 = 2\pi \times 8 \times 10^6 \text{ Hz}$, $J_2 = 2\pi \times 8 \times 10^6 \text{ Hz}$; (d) $g_1 = 2\pi \times 24 \times 10^3 \text{ Hz}$, $g_2 = 2\pi \times 14 \times 10^3 \text{ Hz}$, $G_A = 0 \text{ Hz}$, $J_1 = 2\pi \times 8 \times 10^6 \text{ Hz}$, $J_2 = 2\pi \times 8 \times 10^6 \text{ Hz}$; (e) $g_1 = 2\pi \times 24 \times 10^3 \text{ Hz}$, $g_2 = 2\pi \times 14 \times 10^3 \text{ Hz}$, $G_A = 2\pi \times 8 \times 10^6 \text{ Hz}$, $J_1 = 0 \text{ Hz}$, $J_2 = 2\pi \times 8 \times 10^6 \text{ Hz}$; (f) $g_1 = 2\pi \times 24 \times 10^3 \text{ Hz}$, $g_2 = 2\pi \times 14 \times 10^3 \text{ Hz}$, $G_A = 2\pi \times 8 \times 10^6 \text{ Hz}$, $J_1 = 2\pi \times 8 \times 10^6 \text{ Hz}$, $J_2 = 0 \text{ Hz}$; For all plots, $m = 20 \text{ ng}$, $\omega_m = 2\pi \times 60 \times 10^6 \text{ Hz}$, $\kappa_1 = 2\pi \times 12 \times 10^6 \text{ Hz}$, $\kappa_2 = 2\pi \times 4 \times 10^3 \text{ Hz}$, $\kappa_3 = 2\pi \times 4 \times 10^3 \text{ Hz}$, $\gamma = 2\pi \times 8 \times 10^3 \text{ Hz}$, $Q = 6700$, $\Delta = 1 \times \omega_m$, $\gamma_{m1} = \gamma_{m2} = \omega_m/Q$, $P = 3 \times 10^{-3} \text{ W}$.

are consistent with early studies as reported in (Pan et al.2021). The output spectral lines are symmetrically distributed, and the two transparent windows in the middle are wider. So the existence of the two-level atomic ensemble will benefit our observation of the multi-OMIT phenomenon.

In Fig. 2(e), when the coupling between the cavity fields a_1 and a_2 is switched off ($J_1 = 0$), the characteristics of OMIT also change significantly. We can clearly see three OMIT, and the two outermost transparent windows are the same width. The three transparent windows indicate that the system becomes transparent to the detection field at three different frequencies at the same time. And the pump field and the detection field produce four interference paths (Xiao et al.2020).

In Fig. 2(f), the characteristics of OMIT are similar to the case of $J_1 = 0$, both of them have three OMIT, the absorption line of the probe field presents three dips. But by contrast, it can be noticed that the two spectral lines at $J_2 = 0$ are wider and more dispersed in this system. It has been demonstrated that the spectral responses of the detection fields corresponding to different coupling effects are obviously different.

4 Tunable multiple-OMIT controlled by system parameters

In order to further find the influence of different coupling parameters on the absorption spectrum of the probe field, we take three different sets of data for each coupling factor, and then draw the real part curve of the probe field, which is function of δ/ω_m .

In Fig. 3(a), we simulate the effect of changing coupling strength g_1 between optical cavity a_1 and the charged mechanical resonator b_1 on transparent behavior. When the coupling strength g_1 is not zero, the two outermost transparent windows will split into four. As the coupling increases, the width of the four transparent windows on both sides will gradually increase, and the new transparent points will move outward. Whether g_1 is zero or not, the transparent point in the middle doesn't move, but the width of the transparent window in the middle will change.

In Fig. 3(b), it is found that the overall curve is arranged in an axisymmetric manner. When the coupling between the optical cavity a_3 and the charged mechanical resonator b_2 is switched off, that is, $g_2 = 0$, the curves display three OMIT phenomenon. Particularly, increasing g_2 does not change the position of the middle transparent point, but it makes the middle transparent window wider. Regardless of the value of g_2 , the width of the transparent window width only reaches its maximum value when $g_2 = 0$, and it is located in the middle of the image.

In Fig. 3(c), we investigate the effect of atomic ensemble on OMIT in cavity optomechanical system and change the coupling strength between the atomic ensemble and the cavity field. The number of transparent windows is changed from four to five under the interference of two-level atomic ensemble. This is because the middle transparent window is divided into two. In other words, the two-level atomic ensemble contributes a transparent window to the cavity opto-mechanical system (Ma et al.2014), and the quantum interference occurs between different energy level paths of atoms. More importantly, no matter how the parameters change, all transparent points don't move.

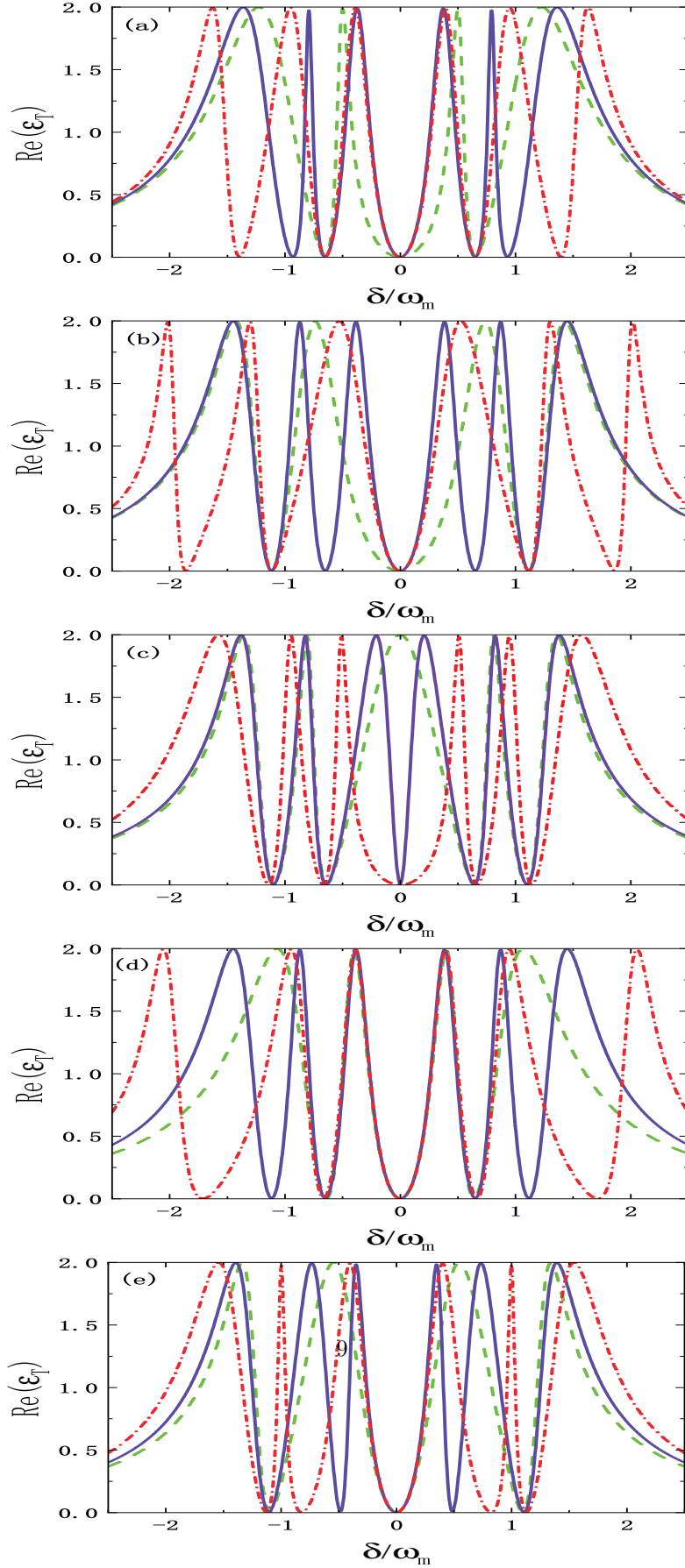


Fig. 3 The image describes the output spectral lines of three sets of data taken by coupling parameters g_1 , g_2 , G_A , J_1 and J_2 , respectively. We use the control variable method so that each image corresponds to the given parameter one by one. The rest of the data are the same as in Fig. 2. (a) $g_1 = 0\text{Hz}$ (green dashed line), $g_1 = 40\pi \times 10^3\text{Hz}$ (blue solid line), $g_1 = 60\pi \times 10^3\text{Hz}$ (red dashed-dotted line); (b) $g_2 = 0\text{Hz}$ (green dashed line), $g_2 = 28\pi \times 10^3\text{Hz}$ (blue solid line), $g_2 = 80\pi \times 10^3\text{Hz}$ (red dashed-dotted line); (c) $G_A = 0\text{Hz}$ (green dashed line), $G_A = 8\pi \times 10^6\text{Hz}$ (blue solid line), $G_A = 24\pi \times 10^6\text{Hz}$ (red dashed-dotted line); (d) $J_1 = 0\text{Hz}$ (green dashed line), $J_1 = 16\pi \times 10^6\text{Hz}$ (blue solid line), $J_1 = 24\pi \times 10^6\text{Hz}$ (red dashed-dotted line); (e) $J_2 = 0\text{Hz}$ (green dashed line), $J_2 = 12\pi \times 10^6\text{Hz}$ (blue solid line), $J_2 = 20\pi \times 10^6\text{Hz}$ (red dashed-dotted line).

In Fig. 3(d), when $J_1 = 0$, three transparent windows are displayed in the image. As the coupling becomes stronger, two new absorption peaks appear in the output field. Specifically, we noticed that the curves of the middle three transparent windows overlap highly and almost do not change with the parameters. As the parameter increases, the width of the two outermost transparent windows will increase, they will also move further and further away from the center. It has been verified by (Pan et al.2021).

In Fig. 3(e), we plot the real part curves of the transmission probe spectrum. It presents the variation of OMIT with δ/ω_m for different coupling strengths J_2 between the optical cavity a_2 and the optical cavity a_3 . The existence of the coupling strength J_2 induces the splitting effect of the transparent window. We can clearly see the middle window split into three. The width of the absorption peaks of the three spectral lines also changes. At the same time, the position of the two newly emerged transparent points in the middle is greatly affected by the coupling effect.

5 Conclusion

In this paper, the physical model of the multi-cavity system is based on the J-C model, and both the cavity field and two-level atomic ensemble are fully quantized. In addition, we have also investigate the influence of various factors on OMIT. When the intensity of one of the coupling actions in a multi-cavity optomechanical system changes, the optical response characteristics of OMIT will also change. The specific expressions are the amount and width of OMIT, and the position of transparent points. When some of interactions disappear, the number of transparent windows will decrease. To bring out prominently the effect of atomic ensemble, we specifically manipulate the coupling constant between the atomic ensemble and the cavity field. The introduction of atomic ensemble contributes a transparent window to the system. We use the quantized model and method to effectively promote the deep integration of photons, phonons, and two-level atomic ensemble. The application of these methods makes phonon storage more flexible and reliable, and also plays a key role in photon information transmission.

- Acknowledgements This study was supported by the Provincial Quality Project of Anhui Higher Education Institution of China (Grant No. 2022xsxx048), the Provincial Natural Science Foundation of Anhui Higher Education Institution of China (Grant No. KJ2020A0331).
- Author contributions GTY: Model conceptualization, simulation calculation, first draft writing. GXP: software, methodology, project administration, supervision.
- Funding The Provincial Quality Project of Anhui Higher Education Institution of China (Grant No. 2022xsxx048), the Provincial Natural Science Foundation of Anhui Higher Education Institution of China (Grant No. KJ2020A0331).
- Availability of data and materials Data from the simulation can be assessed upon request to the authors.

Declarations

- Conflicts of interest Authors declare no competing interests.
- Ethical approval This declaration is not applicable.

References

- Agarwal, G.S., Huang, S.M.: Optomechanical systems as single-photon routers. *Phys. Rev. A* 85, 021801 (2012)
- Akram, M.J., Khan, M.M., Saif, F.: Tunable fast and slow light in a hybrid optomechanical system. *Phys. Rev. A* 92, 023846 (2015)
- Alford, M.G., Harris, S.P.: Damping of density oscillations in neutrino-transparent nuclear matter. *Phys. Rev. C* 100, 035803(13pp) (2019)
- Arregui, G., Ng, R.C., Albrechtsen, M., Stobbe, S., Sotomayor-Torres, C. M., Garc??a, P. D.: Cavity Optomechanics with Anderson-Localized Optical Modes. *Phys. Rev. Lett.* 130, 043802 (2023)
- Bhattacharya, M., Meystre, P.: Multiple membrane cavity optomechanics. *Phys. Rev. A* 78, 041801(4pp)(R) (2008)
- Chen, B., Jiang, C., Zhu, K.D.: Slow light in a cavity optomechanical system with a Bose-Einstein condensate. *Phys. Rev. A* 83, 055803 (2011)
- Chen, B., Shang, L., Wang, X.F., Chen, J.B., Xue, H.B., Liu, X., Zhang, J.: Atom-assisted second-order sideband generation in an optomechanical system with atom-cavity-resonator coupling. *Phys. Rev. A* 99, 063810(8pp) (2019)
- Gebremariam, T., Zeng, Y.X., Mazaheri, M., Li, C.: Enhancing optomechanical force sensing via precooling and quantum noise cancellation. *China-Phys. Mech. Astron.* 63, 210311 (2020)
- Gu, W.J., Yi, Z.: Double optomechanically induced transparency in coupled-resonator system. *Opt. Commun.* 333, 261 (2014)
- Hamed, H.R., Yannopapas, V., Juzeli??nas, G., Paspalakis, E.: Coherent optical effects in a three-level quantum emitter near a periodic plasmonic nanostructure. *Phys. Rev. B* 106, 035419 (2022)
- Hao, X.Z., Zhang, X.Y., Zhou, Y.H., Dai, C.M., Hou, S.C., Yi, X.X.: Topologically protected optomechanically induced transparency in a one-dimensional optomechanical array. *Phys. Rev. A* 105, 013505 (2022)
- Huang, S.M., Tsang, M.: Electromagnetically induced transparency and optical memories in an optomechanical system with N membranes. arXiv: 1403.1340v1 (2014)
- Jiang, C., Jiang, L., Yu, H.L., Cui, Y.S., Li, X.W., Chen, G.B.: Fano resonance and slow light in hybrid optomechanics mediated by a two-level system. *Phys. Rev. A* 96, 053821(8pp) (2017)
- Jing, Y.W., Shi, H.Q., Xu, X.W.: Nonreciprocal photon blockade and directional amplification in a spinning resonator coupled to a two-level atom. *Phys. Rev. A* 104, 033707 (2021) <https://doi.org/10.1103/PhysRevA.104.033707>
- Kharel, P., Chu, Y., Mason, D., Kittlaus, E.A., Otterstrom, N.T., Gertler, S., Rakich, P.T.: Multimode Strong Coupling in Cavity Optomechanics. *Phys. Rev. Applied* 18, 024054 (2022)

- Kien, F. L., Hejazi, S.S.S., Busch, T., Truong, V.G., Chormaic, S.N.: Channeling of spontaneous emission from an atom into the fundamental and higher-order modes of a vacuum-clad ultrathin optical fiber. *Phys. Rev. A* 96, 043859(19pp) (2017)
- Kumar, R., Barrios, E., Kupchak, C., Lvovsky, A.I.: Experimental Characterization of Bosonic Creation and Annihilation Operators damping oscillation. *Phys. Rev. Lett.* 110, 130403(5pp) (2013)
- Kuraptsev, A.S., Sokolov, I.M.: Spontaneous decay of an atom excited in a dense and disordered atomic ensemble: Quantum microscopic approach. *Phys. Rev. A* 90, 012511(7pp) (2014)
- Lai, D.G., Wang, X., Qin, W., Hou, B.P., Nori, F., Liao, J.Q.: Tunable optomechanically induced transparency by controlling the dark-mode effect. *Phys. Rev. A* 102, 023707(17pp) (2020)
- Lai, G.D., Zou, F., Hou, B.P., Xiao, Y.F., Liao, J.Q.: Simultaneous cooling of coupled mechanical resonators in cavity optomechanics. *Phys. Rev. A* 98, 023860(13pp) (2018)
- Lembessis, V. E., Koksals, K., Yuan, J., Babiker, M.: Chirality-enabled optical dipole potential energy for two-level atoms. *Phys. Rev. A* 103, 013106(6pp) (2021)
- Ling, T.X., Mintert, F.: Deterministic preparation of nonclassical states of light in cavity optomechanics. *Phys. Rev. Research* 3, 033071(10pp) (2021)
- Liu, T., Xu, J., Su, Q.P., Zhou, Y.H., Wu, Q.C.: Two-photon process of a single two-level atom simultaneously absorbing or emitting two photons distributed in different cavities and its applications. *Phys. Rev. A* 106, 063721 (2022)
- Lu, H., Wang, C.Q., Yang, L., Jing, H.: Optomechanically induced thermal bistability in an optical microresonator. *Phys. Rev. A* 10, 014006 (2018)
- Lu, T.X., Jiao, Y.F., Zhang, H.L., Saif, F., Jing, H.: Selective and switchable optical amplification with mechanical driven oscillators. *Phys. Rev. A* 100, 013813 (2019)
- Ma, P.C., Zhang, J.Q., Xiao, Y., Feng, M., Zhang, Z.M.: Tunable double optomechanically induced transparency in an optomechanical system. *Phys. Rev. A* 90, 043825(6pp) (2014)
- Oka, H., Takeuchi, S., Sasaki, K.: Optical response of two-level atoms with reflection geometry as a model of a quantum phase gate. *Phys. Rev. A* 72, 013816(7pp) (2005)
- Oliveira, M.H., M??ximo, C.E., Villas-Boas, C.J.: Sensitivity of electromagnetically induced transparency to light-mediated interactions. *Phys. Rev. A* 104, 063704 (2021) <https://doi.org/10.1103/PhysRevA.104.063704>
- Pan, G.X., Xiao, R.J., Chen, H.J., Gao, J.: Multicolor optomechanically induced transparency in a distant nano-electro-optomechanical system assisted by two-level atomic ensemble. *Laser. Physics.* 31 065202(7pp) (2021)
- Pan, G.X., Xiao, R.J., Gao, J.: Enhanced entanglement and output squeezing of optomechanical system via a single four-level atom. *Laser Phys. Lett.* 17, 085204 (2020)
- Safavi-Naeini, A.H., Mayer Alegre, T.P., Chan, J., Eichenfield, M., Winger, M., Lin, Q., Hill, J.T., Chang, D.E., Painter, Q.: Electromagnetically induced transparency and slow light with optomechanics. *Nature.* 472, 69 (2011)

- Sarma, B., Sarma, A.K.: Controllable optical bistability in a hybrid optomechanical system. *J. Opt. Soc. Am. B* 33, 1335 (2016)
- Sohail, A., Zhang, Y., Zhang, J., Yu, C.S.: Optomechanically induced transparency in multi-cavity optomechanical system with and without one two-level atom. *Sci. Rep* 6 28830(8pp) (2016)
- Vlasiuk, E., Poshakinskiy, A.V., Poddubny, A.N: Two-photon pulse-scattering spectroscopy for arrays of two-level atoms coupled to a waveguide. *Phys. Rev. A* 108, 033705 (2023) <https://doi.org/10.1103/PhysRevA.108.033705>
- Watanabe, T.: Effect of dipole-dipole interaction on unpolarized ultracold fermionic gases in a two-dimensional optical lattice. *Phys. Rev. A* 80, 053621(5pp) (2009)
- Wu, S.C., Qin, L.G., Jing, J., Yang, G.H., Wang, Z.Y.: Triple optomechanical induced transparency in a two-cavity system. *Chin. Phys. B* 25, 054203(6pp) (2016)
- Wu, Y., Nie, W.J., Li, G.Y., Chen, A.X., Lan, Y.H.: Thermophonon flux in double-cavity optomechanics. *Phys. Rev. A* 103, 043521(9pp) (2021)
- Xiao, R.J., Pan, G.X., Xiu, X.M.: Controlling multiple optomechanically induced transparency in the distant cavity-optomechanical system. *Chinese. Phys. B* 30, 034209 (2020)
- Xiao, R.J., Pan, G.X., Zhou, L.: Analog multicolor electromagnetically induced transparency in multimode quadratic coupling quantum optomechanics. *J. Opt. Soc. Am. B* 32, 1399 (2015)
- Yan, X.B.: Optomechanically induced transparency and gain. *Phys. Rev. A* 101, 043820(7pp) (2020)
- Yang, X., Brewer, N., Lett, D.P.: Quantum treatment of cavity-assisted entanglement of three-level atoms and two fields in an electromagnetically-induced-transparency configuration. *Phys. Rev. A* 105, 023711 (2022)
- Zeng, Y.X., Shen, J., Gebremariam, T., Li, C.: The study of interference effect in a globally coupled quantum network. *Quantum Inf. Process.* 18, 205 (2019)
- Zhang, D.W., You, C., L??, X.Y.: Intermittent chaos in cavity optomechanics. *Phys. Rev. A* 101, 053851(5pp) (2020)
- Zhang, S., Tian, T.C., Wu, Z.Y., Zhang, Z.S., Wang, X.H., Wu, W., Bao, W.S., Guo, C.: Steady-state phonon occupation of electromagnetically-induced-transparency cooling: Higher-order calculations. *Phys. Rev. A* 104, 013117 (2021b) <https://doi.org/10.1103/PhysRevA.104.013117>
- Zhang, X.Y., Zhou, Y.H., Guo, Y.Q., Yi, X.X.: Optomechanically induced transparency in optomechanics with both linear and quadratic coupling. *Phys. Rev. A* 98, 053802 (2018)
- Zheng, T., Wang, P., Wei, B., Lu, B., Cao, B., Lei, F.: Three-pathway electromagnetically induced transparency and absorption based on coupled superconducting resonators. *Phys. Rev. A* 108, 053105 (2023)
- Zhang, F.Y., Yang, C.P.: Generation of generalized hybrid entanglement in cavity electro?Coptic systems. *Quantum Sci. Technol.* 6, 025003 (2021a)
- Zhang, J.Q., Li, Y., Feng, M., Xu, Y.: Precision measurement of electrical charge with optomechanically induced transparency. *Phys. Rev. A* 86, 053806 (2012)